Design and Operational Assessment of a Low-boom Low-drag Supersonic Business Jet

Yicheng Sun[*], Howard Smith

School of Aerospace Transport and Manufacturing, Cranfield University, Bedford, MK43 0AL, UK

Abstract: There has been a worldwide interest to develop a supersonic business jet (SSBJ) for a minimum range of 4,000 nm with low sonic boom intensity and high fuel efficiency. An SSBJ design model is developed in the GENUS aircraft conceptual design environment. With the design model, a low-boom low-drag SSBJ concept is designed and optimized. This paper studies the design concept for its operational performances. The sustained supersonic cruise flight is studied to find out the fuel-efficient Mach number and altitude combinations. The combined supersonic and subsonic cruise flight scenarios are studied to evaluate the feasibility of boom-free flight routes. The one-stop supersonic cruise flight scenario is studied to compare the fuel consumption and time advantage over subsonic airliners. The off-design sonic boom intensity is studied to explore the operational space assuming there would be a sonic boom intensity limit in the future. Through the studies, it is revealed that there is a corresponding most fuel-efficient operating altitude for a specific cruise Mach number. To operate the aircraft near the cut-off Mach number leads to both increases in the fuel consumption (6.3% - 8.1%) and the mission time (11.7% - 13.1%). The business-class supersonic transport (231 g/PAX/km) consumes nearly three times fuel as the economic-class supersonic transport (77 g/PAX/km), which is still far more than the economic-class subsonic transport (20 g/PAX/km). Off-design sonic boom intensity studies reveal different trends against the common understanding: the sonic boom intensity does not necessarily decrease as the altitude increases; the sonic boom intensity does not necessarily decrease as the Mach number decreases.

Keywords: Multidisciplinary design optimization, Supersonic business jet, Sonic boom, Supersonic cruise, Operational assessment

---

[*]Corresponding author.
E-mail address: Yicheng.sun@cranfield.ac.uk (Y. Sun), Howard.Smith@cranfield.ac.uk (H. Smith)

Nomenclature

a_0	=	ambient sound speed
A	=	ray tube area
A_e	=	equivalent area
A_v	=	Mach plane cross sectional area
C_D	=	total drag coefficient
C_{D_F}	=	friction drag coefficient
$C_{D_{LV}}$	=	lift induced vortex drag coefficient
$C_{D_{wave}}$	=	supersonic wave drag coefficient
C_L	=	lift coefficient
C_F	=	skin friction coefficient
$F(x)$	=	F-function at coordinate x
FF	=	form factor
F_{lift}	=	F-function due to lift
F_{volume}	=	F-function due to volume
l	=	overall aircraft length
L/D	=	lift to drag ratio
$L(x, \theta)$	=	lift on a spanwise strip per unit chordwise length
M	=	flight Mach number
p	=	local overpressure
p_0	=	ambient pressure
psf	=	pound per square foot
q_∞	=	ambient dynamic pressure
r	=	radius in polar coordinate
SFC	=	specific fuel consumption
S_{ref}	=	reference area
S_{wet}	=	wet area

x	=	longitudinal axis location
δp	=	$p - p_0$
β	=	$\sqrt{M^2 - 1}$
γ	=	ratio of specific heat, 1.4 for air
θ	=	angle between the Y-axis and a projection onto the Y-Z plane of a normal to the Mach plane
χ	=	$x - \beta r$, the location on the axis of the equivalent body of the Mach plane translated field point

1. Introduction

The supersonic civil transport aircraft is unique in the civil aviation history. It has been over 50 years since the first flight of Concorde, which retired in 2003 due to the high operating costs and the rising environmental concerns (sonic boom, noise, emissions, etc.). It is widely recognized that the biggest challenges for civil supersonic transport are sonic boom disturbance and high fuel consumption[1]. There has been a renewed interest in designing environmentally friendly, economically viable and technologically feasible aircraft for the next-generation supersonic civil transport, of which the pioneer is considered to be the supersonic business jet (SSBJ)[2]. SSBJ is smaller in size and mass, resulting in a lower sonic boom level. It is reasonable to assume that the business jet users (such as executives or heads of state) are more willing to pay for a timesaver. However, the future supersonic civil transport can be viable only if overland supersonic restrictions are relaxed or entirely lifted[3]. There have been studies on low-boom low-drag supersonic transport[4, 5]. Accordingly, NASA is working on the experimental Quiet Supersonic Technology X-59[6] to support the potential change in FAA (Federal Aviation Administration) regulations, which bans supersonic flight over land. Besides the sonic boom intensity, the supersonic aircraft are desired to be more efficient in fuel consumption, thus a lower operating cost and emissions. JAXA (Japanese Aerospace Exploration Agency) has been conducting experiments[7-9] to help develop the low-drag supersonic transport. Aerion Supersonic has been updating its supersonic natural laminar flow wing concept[10] to get a higher cruise aerodynamic efficiency. BOOM Technology[11] is developing a 55-seat supersonic passenger airliner with lower ticket price.

Currently, most of the efforts focus on the development of a technical feasible supersonic transport concept, few of them study the operational performance of a design. Gonzalez[12] studies the influence of the flight profile but puts main focus on the climb segments. Gonzalez-Gallego et al.[13] study the trade-offs of subsonic and supersonic combined flight profiles, but their studies are based on a simple research model and there is a lack of sonic boom performance

assessment. Liebhardt et al.[14] study the full-permit, mixed-permit and no-permit flight scenarios and conclude the cut-off Mach number is a valuable asset for supersonic operations. Li et al.[15] study two different over-water routers for two different designs. The International Council on Clean Transport (ICCT) study the environmental noise and emissions standards of supersonic transport in the SUAVE (Stanford University Aerospace Vehicle Environment) environment and suggest the policymakers to establish new environmental standards for supersonic transport[16]. For off-design conditions, Lazzara et al.[17] reveals the perturbations of angle of attach and Mach number would have an impact on the ground boom signature. This paper intends to show the feasibility of low-boom low-drag supersonic designs in a more general multidisciplinary perspective, to study the fuel conservation operating scenarios, and to explore the sonic boom avoidance or constrained overland flight profiles.

The structure of the paper is as follows. The MDAO environment to design and analysis the supersonic concepts is described in Section 2. Section 3 presents the design results of a low-boom low-drag SSBJ and the design methods employed. The operational assessments of the SSBJ concept are detailed and discussed in Section 4. Finally, the conclusions and future work are drawn in Section 5.

2.   Multidisciplinary Design Analysis and Optimization Environment

The research is conducted in a multidisciplinary design analysis and optimization (MDAO) environment called GENUS[18]. It is the aim of the GENUS aircraft conceptual design environment is to provide a modular, flexible framework both for designers to use existing, and for researchers to develop new, or use existing methods for aerospace vehicle design. GENUS is independent of commercial codes and is coded in JAVA, sequentially running on one single core. After evaluating various design systems, nine essential modules and a special module are identified, as shown in Fig. 1. The environment can synthesize and analyze most aerospace vehicle concepts. The modules are linked together tightly, which makes the multidisciplinary design analysis and optimization possible. GENUS has shown its capabilities through a solar UAV (unmanned aerial vehicle) design[19], a hypersonic transport design[20], a blended-wing-body airliner design[21], a conventional airliner design[22] and a combat UAV design[23].
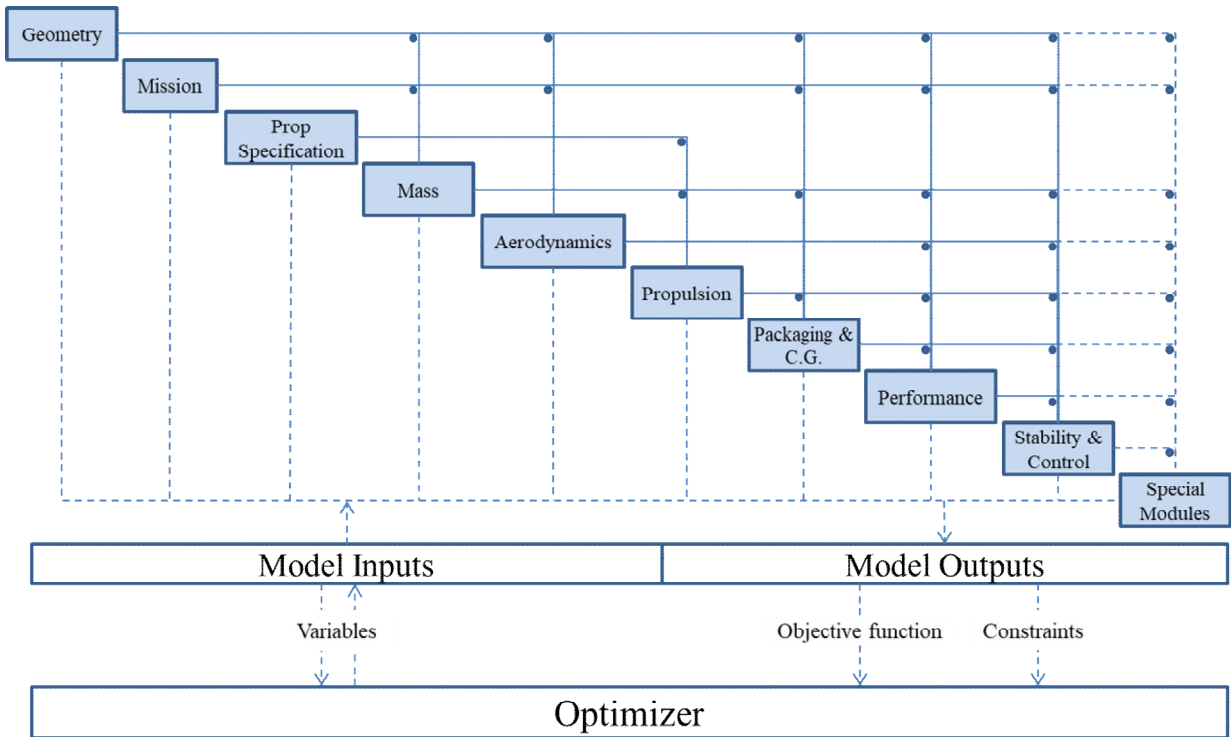
Fig. 1 Structure and data flow of GENUS aircraft design environment

3. SSBJ Design Case

The main challenges for supersonic aircraft design are the sonic boom at ground level and low supersonic efficiency at cruise. The sonic boom can be avoided below the cut-off Mach number (around Mach 1.15), however, the time advantage at this Mach number is not evident. Through the previous studies, the authors have established a multidisciplinary methodologies for supersonic transport[24], validated the design model against different designs[25], demonstrated the sonic boom can be shaped by tailoring the lift and volume distribution[26], and proved the feasibility of low-boom and low-drag design optimization[27]. Therefore, all the previous efforts make the design of a low-boom low-drag SSBJ concept possible. Furthermore, this paper will study the operational performances of an SSBJ concept to help gain more in-depth understanding on the supersonic transport, especially the sonic boom intensity and fuel efficiency. This part introduces the design from a multidisciplinary view.

3.1. Design Mission

The mission module specifies the flight requirements for a design. These requirements are derived from the market or customer specifications. The mission requirements, shown in Table 1, for SSBJs have been analysed by the authors

in a review paper[1], considering the environmental impacts, technological challenges, and market analysis. They are assumed to be the appropriate initial requirements for environmentally friendly and economically viable SSBJs.

Table 1 SSBJ mission requirements

Requirement	Value	Reference Value[1]
Estimated maximum take-off mass (kg)	45,000	-
Cruise altitude (m)	15,000	<17,000
Cruise Mach	1.8	1.4-2.0
Target range (nm)	4,500	4,000-4,500
Passenger number	10	8-12
Crew number	2	-
Take-off distance (m)	3,000	-
Landing distance (m)	2,200	-

3.2. General Geometry Layout

The geometry parts are abstracted into lifting surface and body component arrays. The lifting surface array is then specified as a wing, horizontal tail, vertical tail or canard. The body component array is specified as a fuselage, engine pod, external tank or tail boom. In this way, the geometry module can represent most of the configurations. The authors have analysed several different wing and fuselage combinations in a previous study[26] and find that a low-boom low-drag design should have uniform longitudinal volume and lift distributions. The fuselage is expected to be slenderer and a highly-swept wing is expected to flat the lift distribution. Horizontal tail is preferred rather than the canard because horizontal tail can help to reduce sonic boom signature in the aft part. The SSBJ concept geometry is shown in Fig. 2.
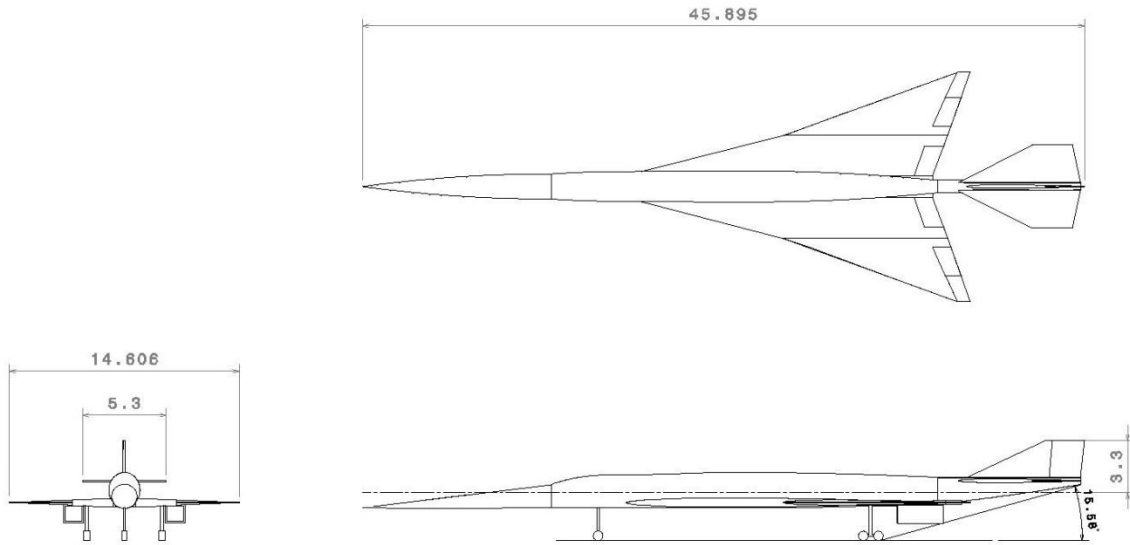
Fig. 2 General arrangement of the SSBJ design

3.3. Aerodynamics

The main aerodynamic analysis tool is PANAIR (panel aerodynamics)[28]. PANAIR can predict inviscid subsonic and supersonic flows of arbitrary configurations by solving a linear partial differential equation numerically. There are several studies[29-31] on supersonic transport applying the PANAIR method and its accuracy is believed to be sufficient for conceptual design. For aerodynamic analysis, PANAIR can provide lift coefficients and induced drag coefficients. The drag components for supersonic flight are denoted by Eq. **(1)**.

$$C_D = C_{D_F} + C_{D_{wave}} + C_{D_{LV}} \tag{1}$$

where C_D is the total drag coefficient, C_{D_F} is the friction drag coefficient, $C_{D_{wave}}$ is the supersonic wave drag coefficient, $C_{D_{LV}}$ is the lift induced vortex drag coefficient.

The form factor method[32] is modified to calculate the zero-lift skin friction and form drag. The result comes from the contribution of each component, as shown in Eq. (2)

$$C_{D_F} = \sum_{j=1}^{N} \frac{FF_j C_{F_j} S_{wet_j}}{S_{ref}} \tag{2}$$

where N is the number of geometric components used to model the configuration, FF_j is the form factor of component j, C_{F_j} is the skin friction coefficient of component j, S_{wet_j} is the wet area of component j, S_{ref} is the reference area of the total aircraft.

The supersonic area rule[33] is applied to calculate wave drag due to volume, as indicated in Eq. (3) and Eq. (4). For accurate wave drag calculation, the Mach plane cross sectional area intersecting with the geometry is required.

$$C_{D_{wave}}(\theta) = -\frac{1}{2\pi} \int_0^l \int_0^l A''(x_1)A''(x_2) \ln|x_1 - x_2| \, dx_1 dx_2 \tag{3}$$

$$C_{D_{wave}} = \frac{1}{2\pi} \int_0^{2\pi} C_{D_{wave}}(\theta) d\theta \tag{4}$$

where θ is the angle between the Y-axis and a projection onto the Y-Z plane of a normal to the Mach plane, l is the overall aircraft length, $A(x)$ is the ray tube area at longitudinal coordinate x.

The drag components and drag polar is plotted in Fig. 3 and the surface pressure distribution is given in Fig. 4.
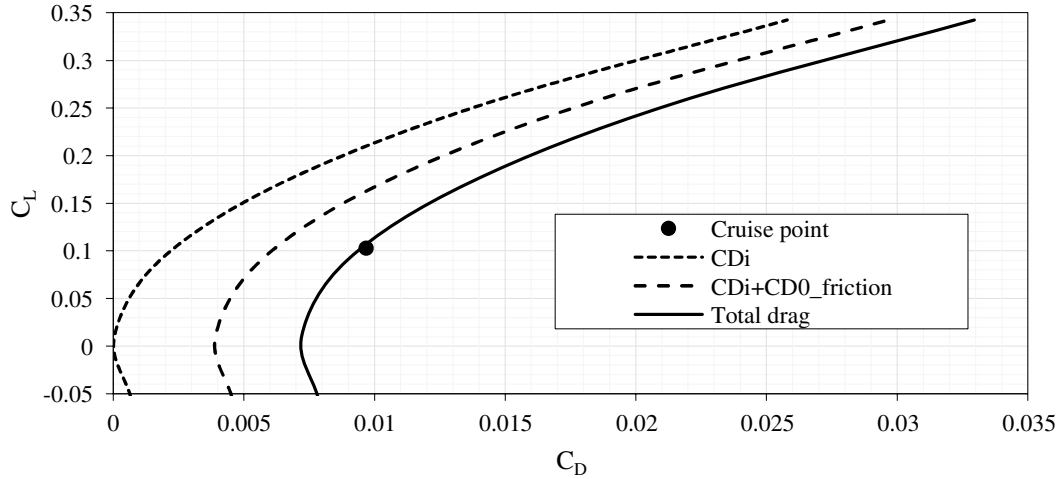
Fig. 3 SSBJ drag components and drag polar
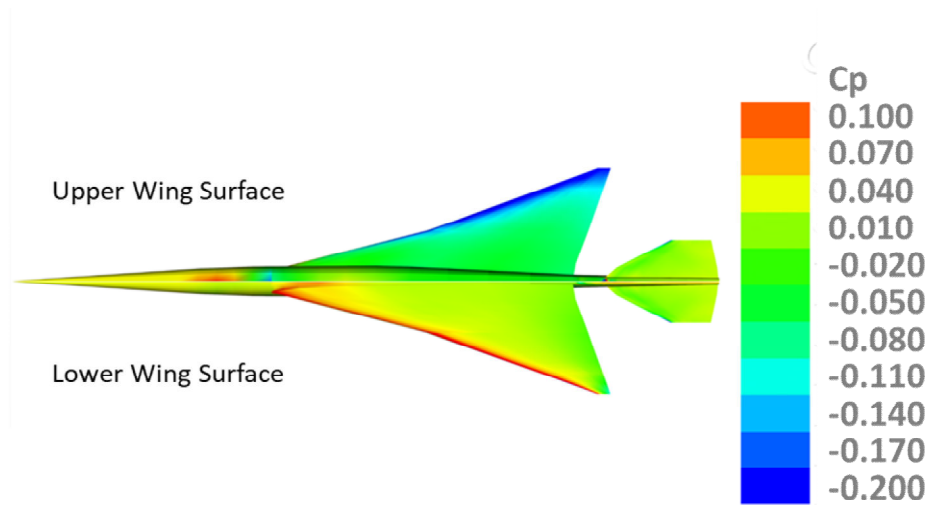
Fig. 4 Wing upper and lower surface pressure distribution

3.4. Propulsion System

The propulsion module uses the NASA EngineSim model[34] to build a rubber engine system. There are four types of engines that EngineSim can design: a turbojet, a turbojet with afterburner, a turbofan, and a ramjet. EngineSim calculates these engines based on the geometry, material properties, flight conditions, throttle setting and so on. A low-bypass turbofan engine, which is the design for the SSBJ concept, is within the design capability of EngineSim. The design parameters, cruise thrust and SFC (specific fuel consumption) of the engine are shown in Table 2.

Table 2 Turbofan engine parameters

Parameters	Value
Bypass ratio	0.4
Diameter (m)	1.075
Length (m)	1.441
Cruise thrust (kN)	21.27
Cruise SFC (g/kN/s)	47.74

3.5. Performance

The performance module is designed to flexibly assemble different segments, which consist of various types of climb, cruise, descent methods. Each segment consists of a number of control points, which are continuous in Mach

number, angle of attack, aerodynamic coefficients, etc. To keep the continuity between segments, the end point of the last segment is set to be the starting point of the next segment. In the later operational assessments, the supersonic and subsonic cruise segments combination and one-stop profile are manipulated in this module.

3.6. Sonic Boom Near-field Pressure

The Whitham theory[35] is used for the near-field pressure calculation. The equivalent area due to volume and equivalent area due to lift are required for the near-field pressure calculation. The equation for the total effective area calculation is indicated in Eq. (**5**).

$$A_e(x, \theta) = A_v(x, \theta) + \frac{\beta}{2q_\infty} \int_0^x L(x, \theta) dx \qquad (5)$$

where $A_e(x, \theta)$ is the equivalent area at coordinate x and angle θ, $A_v(x, \theta)$ is the Mach plane cross sectional area at coordinate x and angle θ, $\beta = \sqrt{M^2 - 1}$, q_∞ is the ambient dynamic pressure, $L(x, \theta)$ is the lift on a spanwise strip per unit chordwise length.

The F-function derives from the equivalent area, as shown in Eq. (**6**).

$$F(x) = \frac{1}{2\pi} \int_0^x \frac{A_e''(\overline{x}, \theta)}{\sqrt{x - \overline{x}}} d\overline{x} \qquad (6)$$

where $F(x)$ is the F-function.

In this research, the F-function is decomposed to F-function due to volume and F-function due to lift, as indicated by Eq. (**7**). This helps to study their individual effects on sonic boom intensity, as plotted in Fig. 5.

$$F(x, \theta) = F_{volume}(x, \theta) + F_{lift}(x, \theta) = \frac{1}{2\pi} \int_0^x \frac{A_v''(\overline{x}, \theta)}{\sqrt{x - \overline{x}}} d\overline{x} + \frac{\beta}{4\pi q_\infty} \int_0^x \frac{L'(\overline{x}, \theta)}{\sqrt{x - \overline{x}}} d\overline{x} \qquad (7)$$

where F_{volume} is the F-function due to volume, F_{lift} is the F-function due to lift.

The near-field pressure is then calculated based on the Whitham theory, as shown in Eq. (**8**).

$$\delta p(x) = p_0 \frac{\gamma M^2 F(\chi)}{(2\beta r)^{1/2}} \qquad (8)$$

where $\delta p = p - p_0$, p_0 is the ambient pressure, γ is the ratio of specific heat, M is the flight Mach number, r is the radius in polar coordinate.

The near-field pressure is optimized through the shaped sonic boom technology by varying the wing and tail planes geometry and positions with essential performance constraints. The F-functions and near-field pressure are plotted in Fig. 5.
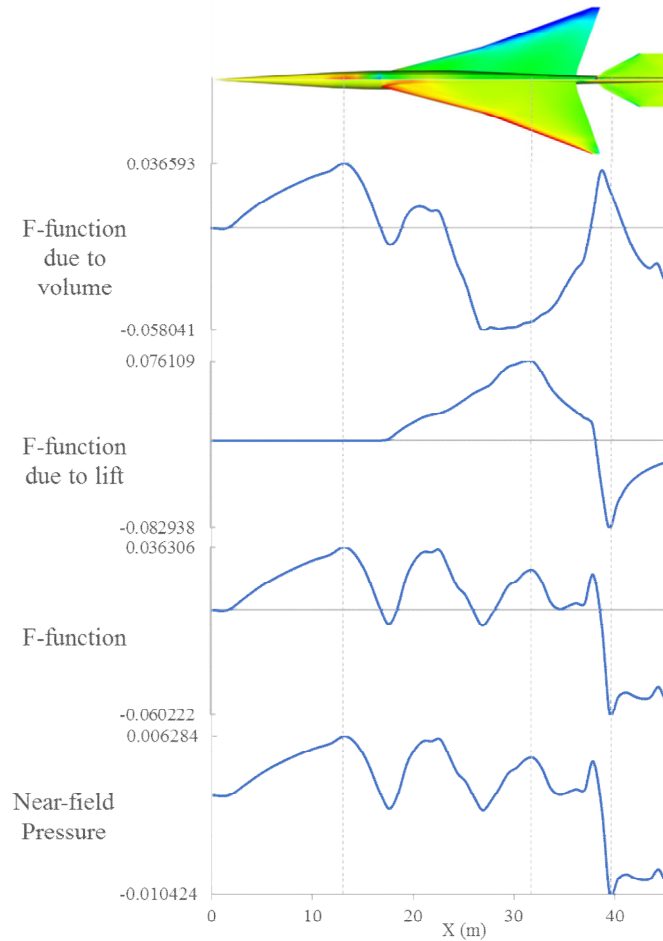
Fig. 5 Near-field pressure generation

3.7. Sonic Boom Ground Signature

Waveform parameter method[36] is based on geometrical acoustics. This method calculates the sonic boom signature directly with distance steps along a ray, which is more suitable for automatic computation. It is reprogrammed in JAVA and implemented as a special module method. A weakness of the method is that the code expects one shock formation or coalescence at a time. For a complex signature with large numbers of points specified, there is a big chance of failure. This becomes a problem when using CFD (computational fluid dynamics) data as F-function inputs. The ground sonic boom signature is plotted in Fig. 6. It can be seen that the peaks of the near-field pressure and the ground signature are corresponding, which is very important for the low-boom design and analysis.
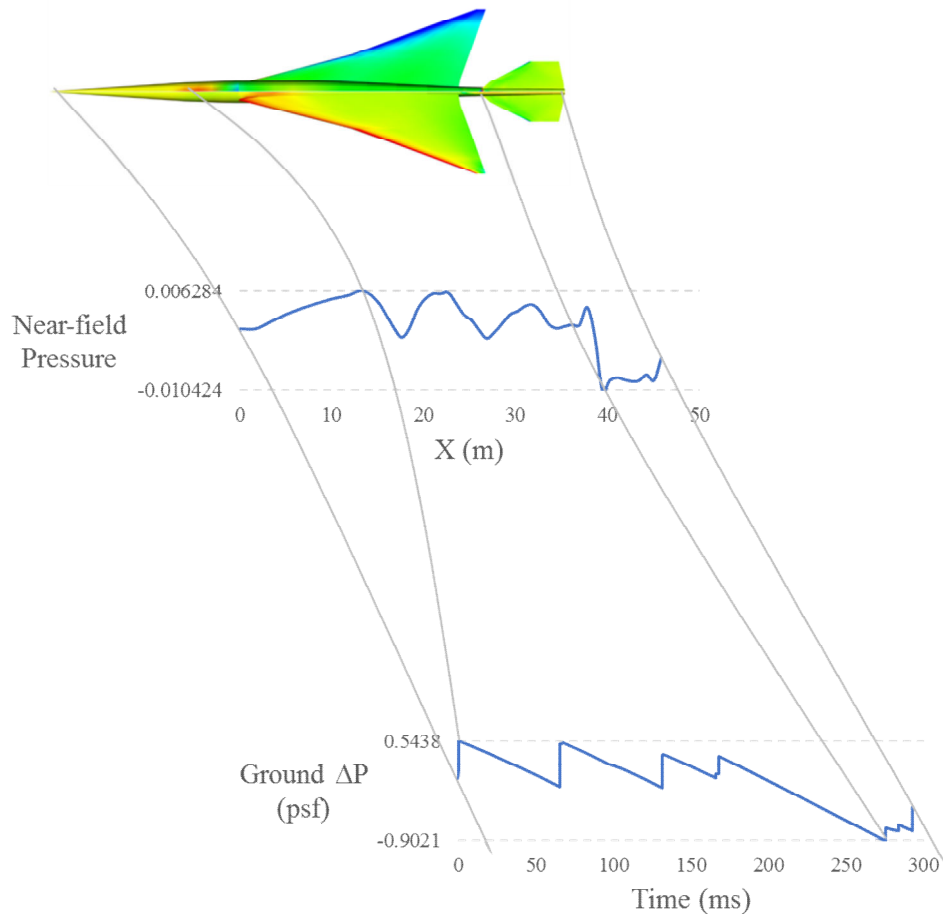
Fig. 6 Sonic boom propagation

4. Operational Assessments

This section gives several trade-off studies of a 10-passenger SSBJ concept in terms of the operational performance. Since the cruise segment has the biggest influence on the mission performance, it is mainly studied in this part. Firstly, the sustained supersonic cruise flight is studied to find out the most fuel-efficient Mach number and altitude combination. Then, different combinations of supersonic and subsonic cruise flights are studied to gain understanding of the boom-free flight routes. Thirdly, the one-stop supersonic cruise flights are studied to compare the fuel consumption and time advantage over subsonic airliners. Lastly, the off-design sonic boom intensity study explores the operational space assuming there is an acceptable sonic boom intensity limit in the future.

4.1. Sustained Supersonic Cruise Flight

This section studies the fuel consumption for sustained supersonic cruise flights at different Mach numbers and altitudes. Fig. 7(a) and Fig. 7(b) plot the flight profiles at cruise Mach 1.8, cruise altitude 13000 m, and cruise Mach 1.8, cruise altitude 19000 m, respectively.

(a)   (b)
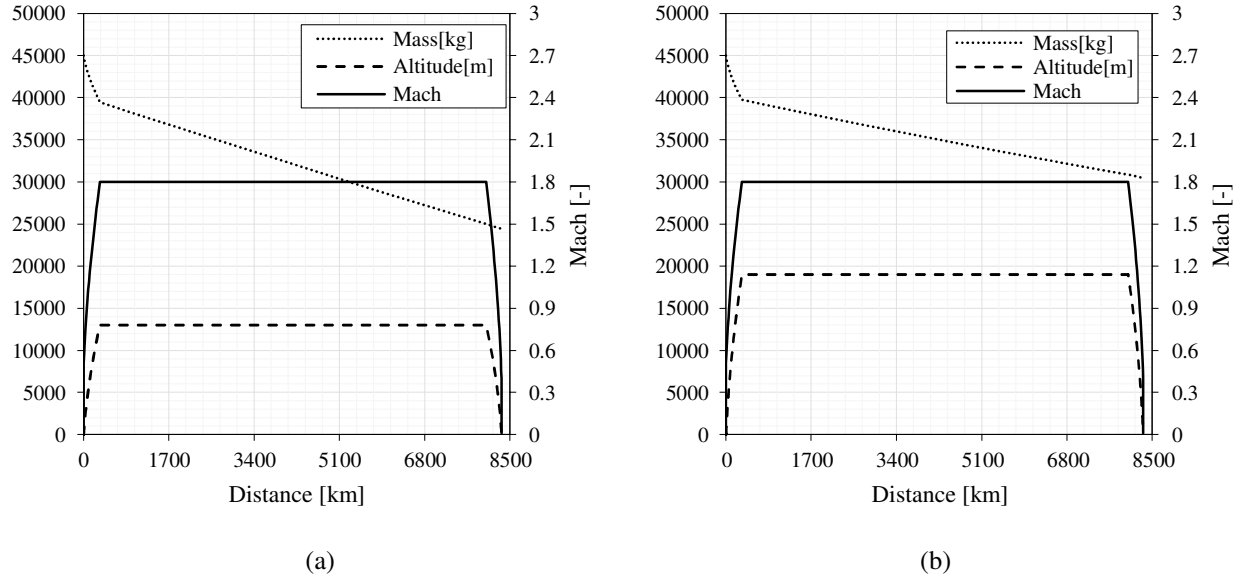
Fig. 7 Mass, altitude and Mach number changes with flight distance for sustained supersonic cruise (a) cruise Mach 1.8, cruise altitude 13000 m; (b) cruise Mach 1.8, cruise altitude 19000 m

The overall fuel consumptions at Mach numbers and altitudes combinations are plotted in Fig. 8. It can be seen from the figure, for each cruise Mach number, there is a range of altitudes where the fuel consumption is at its lowest. This gives the corresponding fuel-efficient altitudes for different operational Mach numbers.
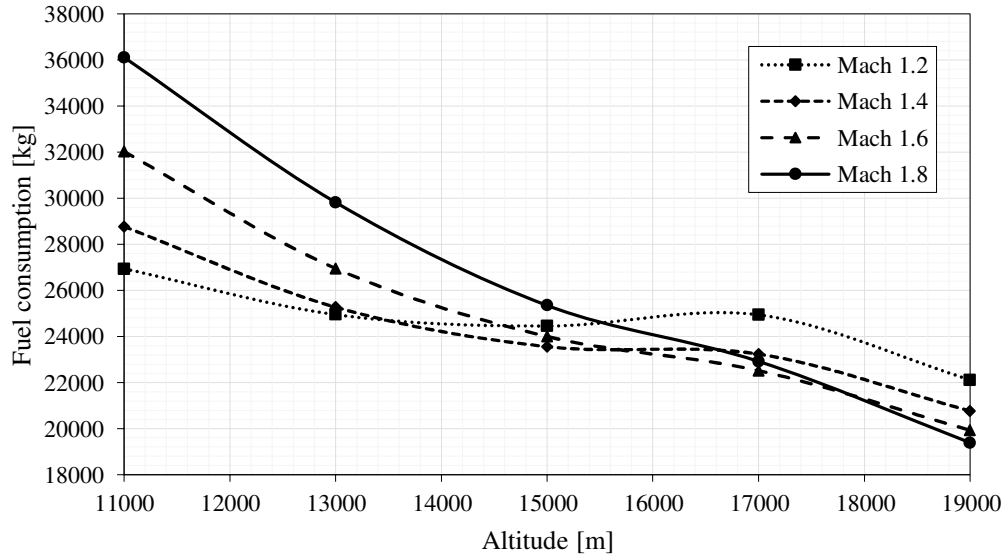
Fig. 8 Fuel consumption at different altitudes and Mach numbers

Here is the explanation for the results in Fig. 8. As indicated by Eq. **(9)**, for the same range and mass, the fuel is proportional to the factor $\frac{SFC}{Mach \times L/D \times a_0}$. For the altitudes (11000 to 19000 m) studied, the speed of sound is the same.

Therefore, the fuel consumption is dominated by the factor $\frac{SFC}{Mach \times L/D}$.

$$Fuel = time \times SFC \times thrust = \frac{range}{Mach \times a_0} \times SFC \times \frac{mass}{L/D} \propto \frac{SFC}{Mach \times L/D \times a_0} \qquad (9)$$

where SFC is the specific fuel consumption, a_0 is the ambient sound speed, L/D is the lift to drag ratio.

The fuel consumption factors are plotted in Fig. 9, which shows the same results as Fig. 8.

(a)

(b)

(c)
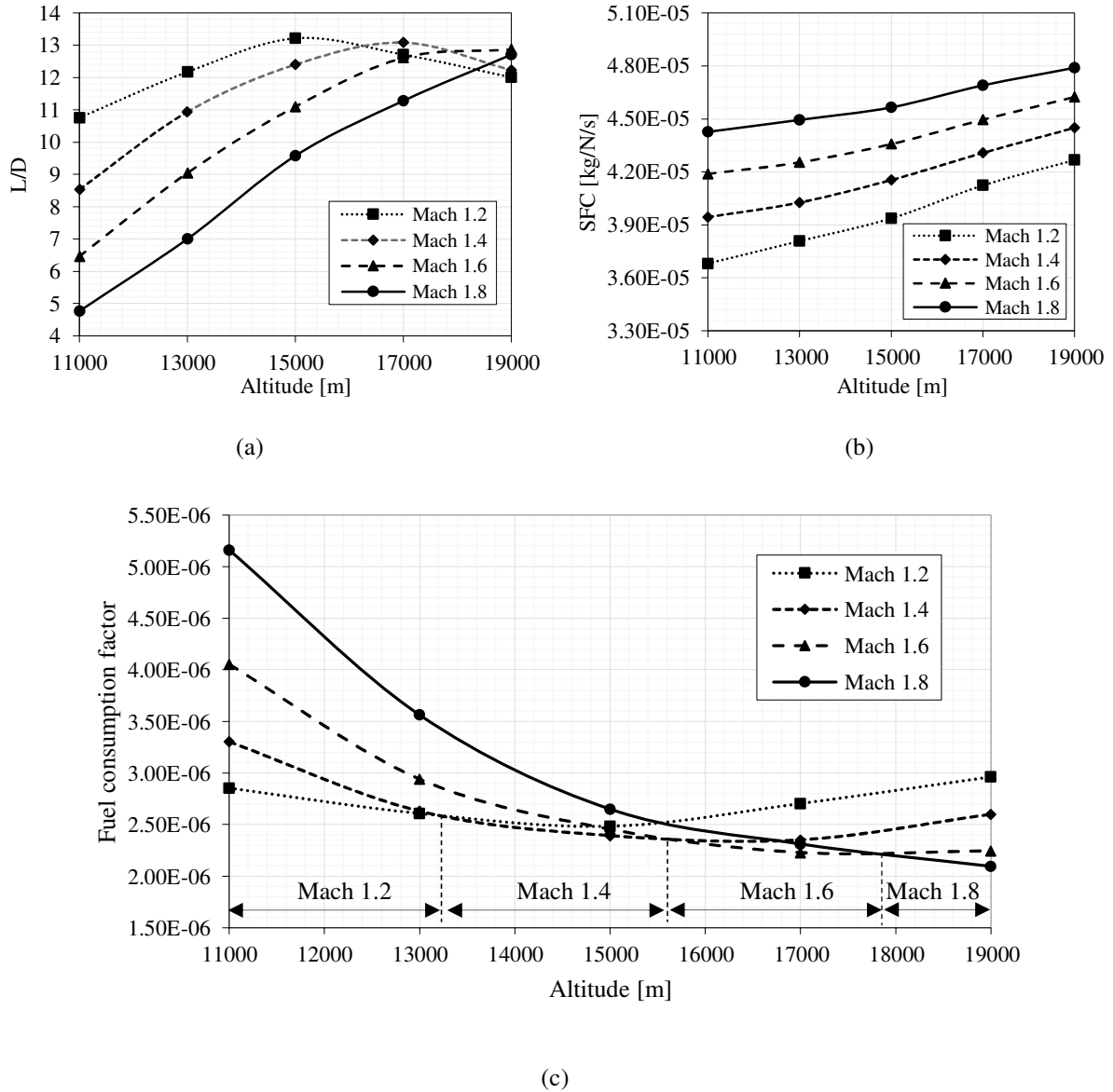
Fig. 9 (a)Lift to drag ratio; (b) specific fuel consumption; (c) fuel consumption factor and fuel-efficient Mach number

The above trade-off studies indicate that there is a fuel-efficient altitude for a specific cruise Mach number. For example, the fuel-efficient altitude for Mach 1.20 is between 11,000m and 13,200 m. For a fixed design, there can be a more detailed plot to indicate the most efficient cruise altitude for each Mach number, as illustrated by Fig. 10. There is an operational feasible zone with the maximum fuel capacity limit. However, the design point is not actually the most fuel-efficient combination of Mach and altitude. If the design point changes, the whole operational plot will

change accordingly. Further work still requires to explore the coordination of the design point and the most fuel-efficient point.
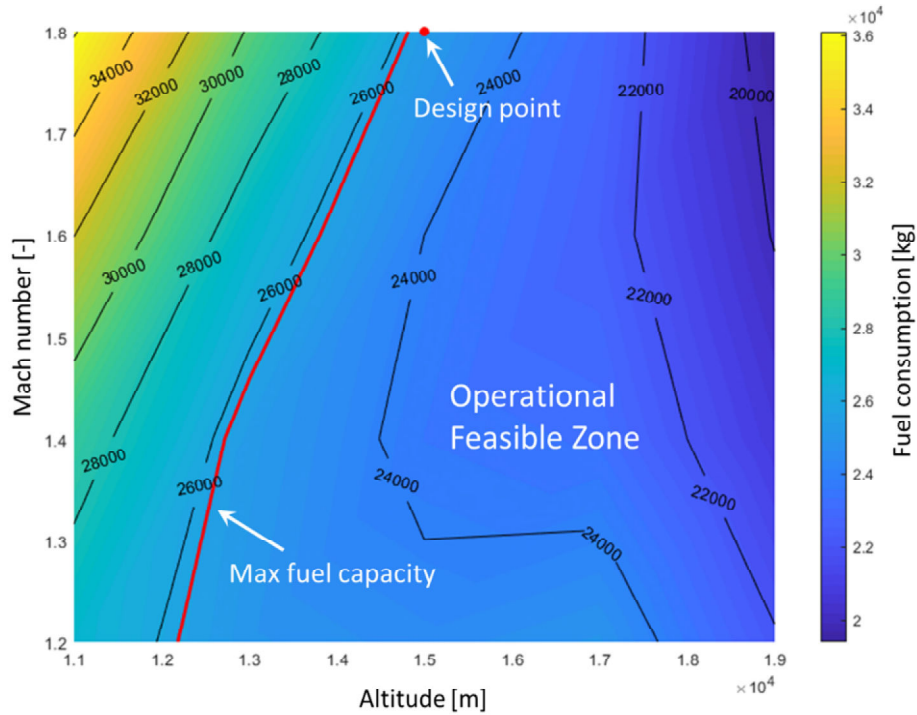
Fig. 10 Different Mach and altitude operational feasible zone with maximum fuel capacity

4.2. Combined Supersonic and Subsonic Cruise Flight

For a specific design, there is an operational scenario to meet the current regulations that ban civil supersonic flight overland. That is to fly at supersonic speeds over sea to maintain the speed advantage and to fly below the cut-off Mach number (around Mach 1.15) over land to avoid sonic boom. In practice, this flight profile can be applied to, for example, a trans-Atlantic route where the initial and final flights are over land. The trans-Atlantic route is one representative case for the 4500 nm range. It is also one of the busiest routes for business travel and the route that Concorde operated. The purpose of this section is to study the performance of the supersonic and subsonic combination flight profile that comply the current regulations, which ban supersonic flight overland.

The SSBJ10 design mission total range for the is 4500nm, of which 1000nm is subsonic cruise range. The subsonic flight is at the normal subsonic airliners cruise altitude (around 11km). A cut-off supersonic Mach number 1.15 and a low supersonic Mach number 1.20 are also studied. The mission profile examples for a combination of Mach 1.80 and Mach 0.80 and a combination of Mach 1.80 and Mach 1.20 are plotted in Fig. 11(a) and Fig. 11(b), respectively.
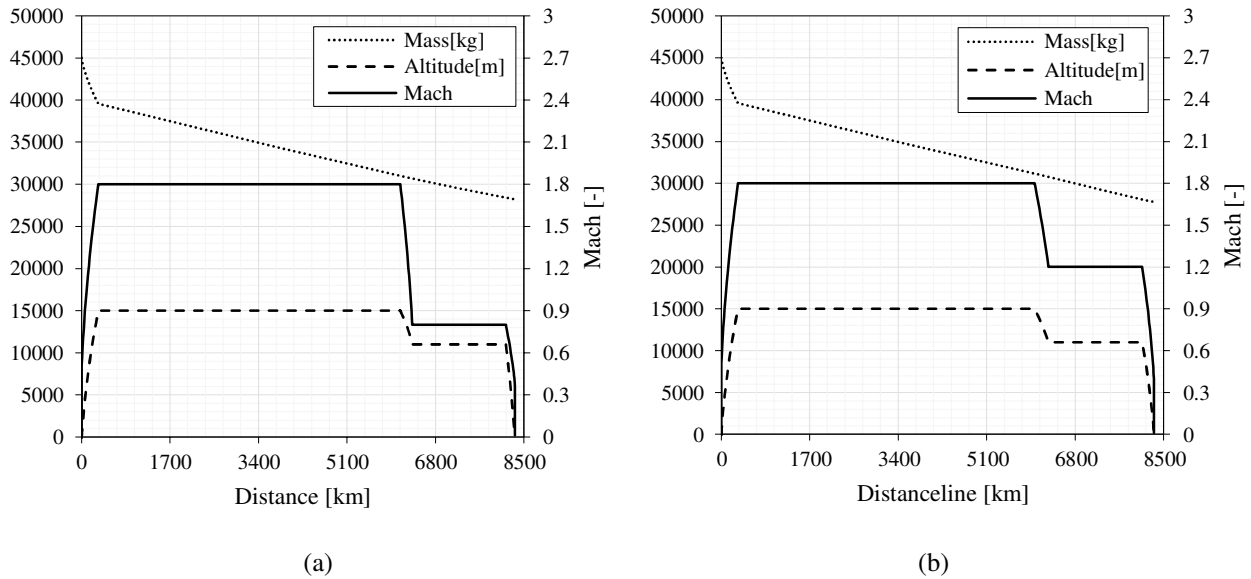
Fig. 11 Mass, altitude and Mach number changes for supersonic and subsonic cruise combinations (a) a combination of Mach 1.80 and Mach 0.80; (b) a combination of Mach 1.80 and Mach 1.20

The overall performance at different Mach numbers are plotted in Fig. 12. It can be noticed that the subsonic cruise segment lead to a reduction in the total fuel consumption (5.0% - 6.8%). However, there will be a significant mission time increase (20.8% - 28.5%). The low supersonic cruises (near the cut-off Mach number) lead to increases both in the mission time (11.7% - 13.1%) and the fuel consumption (6.3% - 8.1%), resulting in a shorter mission range. Therefore, it is advised not to cruise the supersonic aircraft near the cut-off Mach number region, if the design point is not in that region.
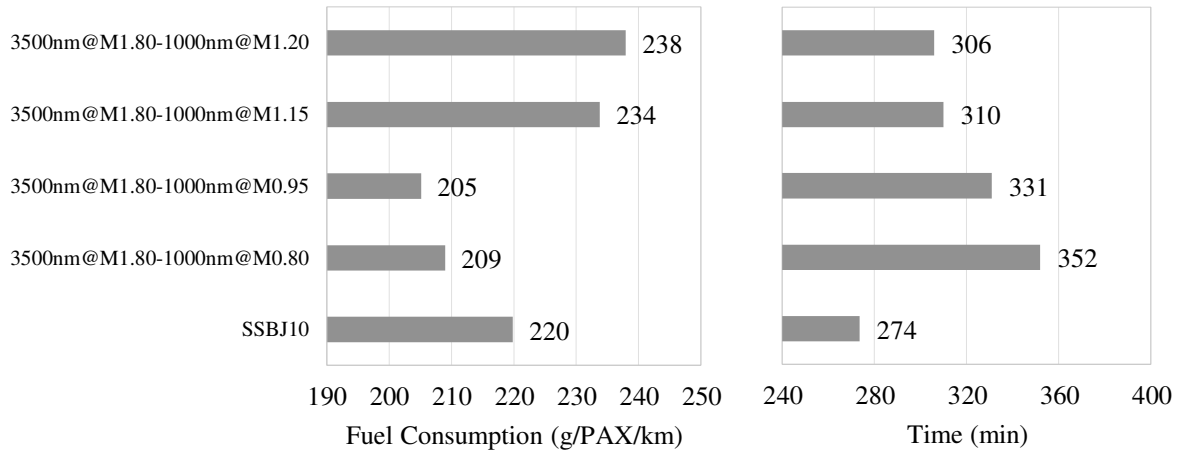
Fig. 12 Fuel consumption and time for different supersonic and subsonic combination flights

From the above analysis, it can be seen that the supersonic and subsonic cruise combinations are fuel-efficient. The subsonic cruise range and Mach number with the maximum design fuel capability is plotted in Fig. 13. Though the complex of the transonic flow might influence the accuracy of the results, a low supersonic cruise subsegment is beyond the operational feasible zone. For different subsonic subsegment range mission, there is a corresponding fuel-efficient Mach number.
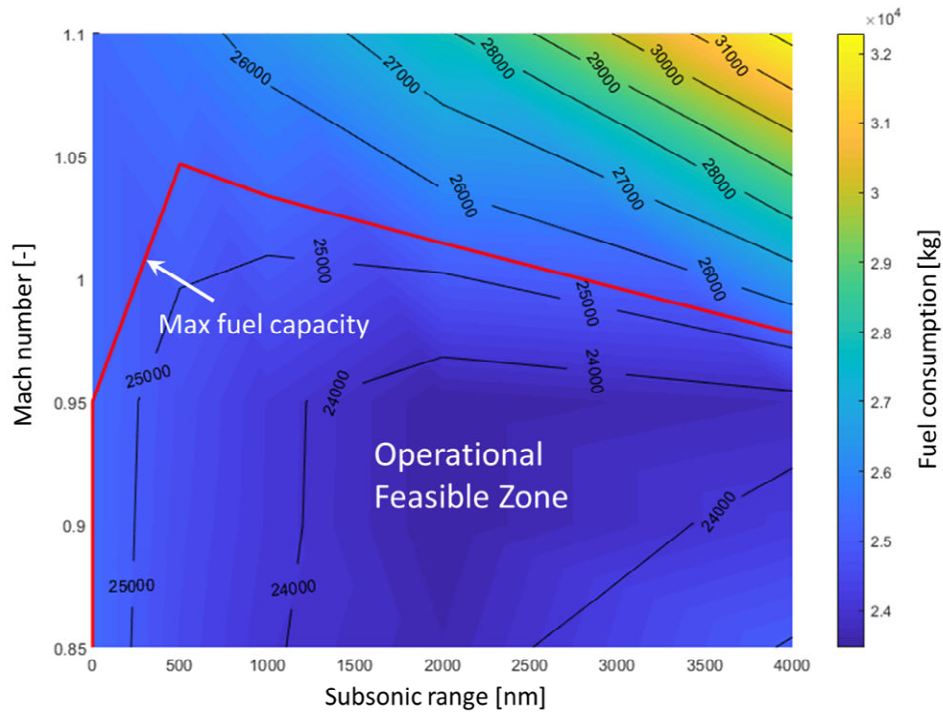
Fig. 13 Subsonic cruise operational feasible zone with maximum fuel capacity

4.3. One-Stop Supersonic Cruise Flight

This part studies the long-range (more than the SSBJ design range 4500nm) flight mission operated by sustained subsonic flights and one-stop supersonic flights. The representative routes for this operation would be the trans-Pacific routes, where the refueling stop can be Honolulu or Adak. Fig. 14(a) and Fig. 14(b) illustrate a 7000nm one-stop mission profile of the supersonic flight over time and over range, respectively. The time lapse for refueling is assumed to be 60 minutes.
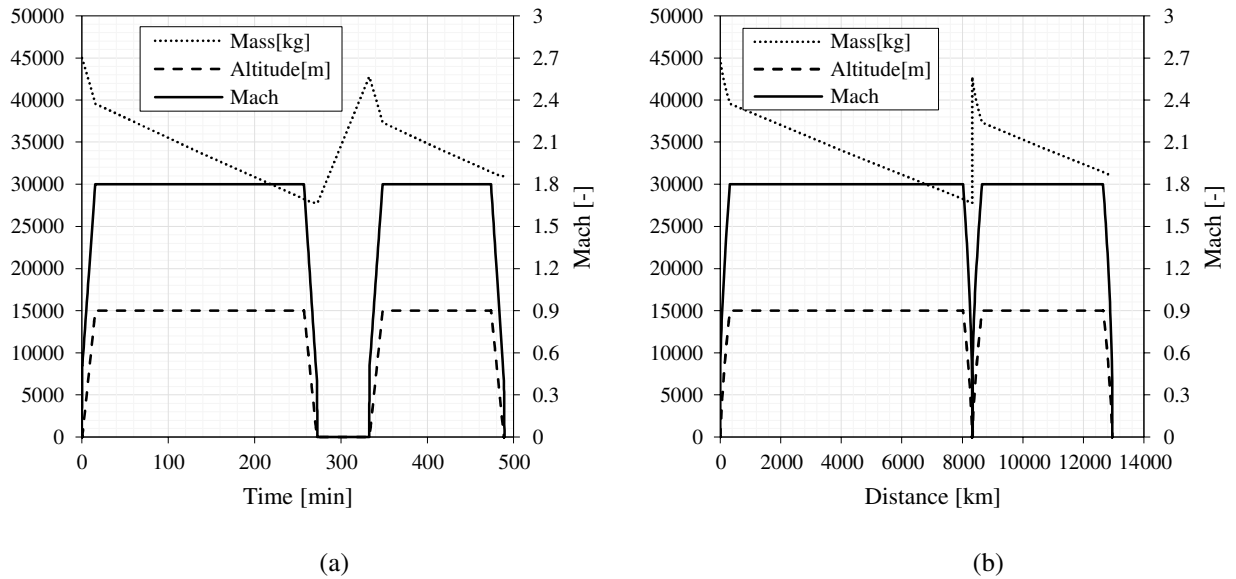
Fig. 14 Mass, altitude and Mach number changes for one-stop supersonic cruise mission trajectory (a) timeline; (b) distance line

The results of fuel consumption and mission time are given by Fig. 15. Not surprisingly, the subsonic airliner has the lowest fuel consumption (20 g/PAX/km). The business class supersonic transport (231 g/PAX/km) consumes three times as much as a supersonic airliner (77 g/PAX/km), which is close to a business class subsonic airliner (81 g/PAX/km). The advantage of supersonic flights is also quite obvious, saving about half (47% - 53%) of the journey time.
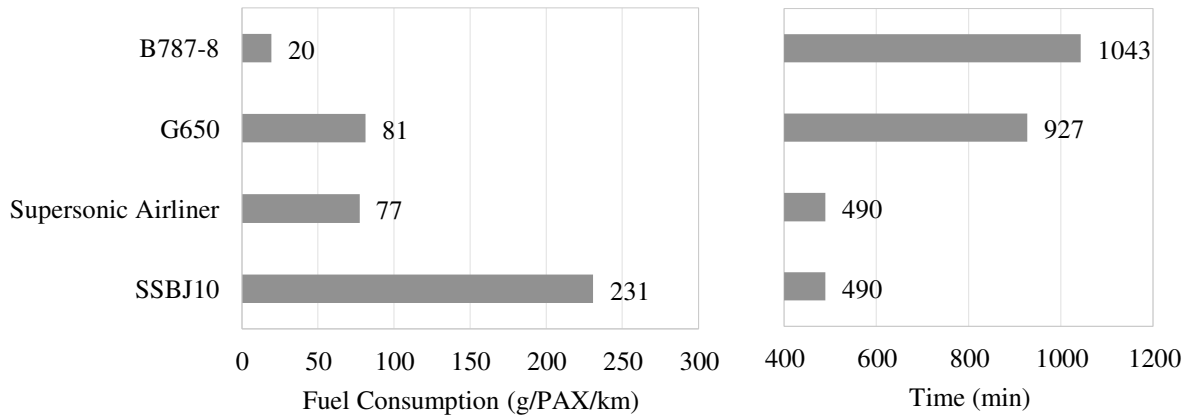

Fig. 15 One-stop supersonic cruise performance for a 7000 nm mission

4.4. Sonic Boom Intensity

This section studies the off-design sonic boom intensity of a fixed design at different Mach numbers and altitudes. The overall sonic boom performance is plotted in Fig. 16. Here are two trends that against the common understanding. Firstly, the sonic boom intensity does not necessarily decrease as the altitude increases. Secondly, the sonic boom intensity does not necessarily decrease as the Mach number decreases.
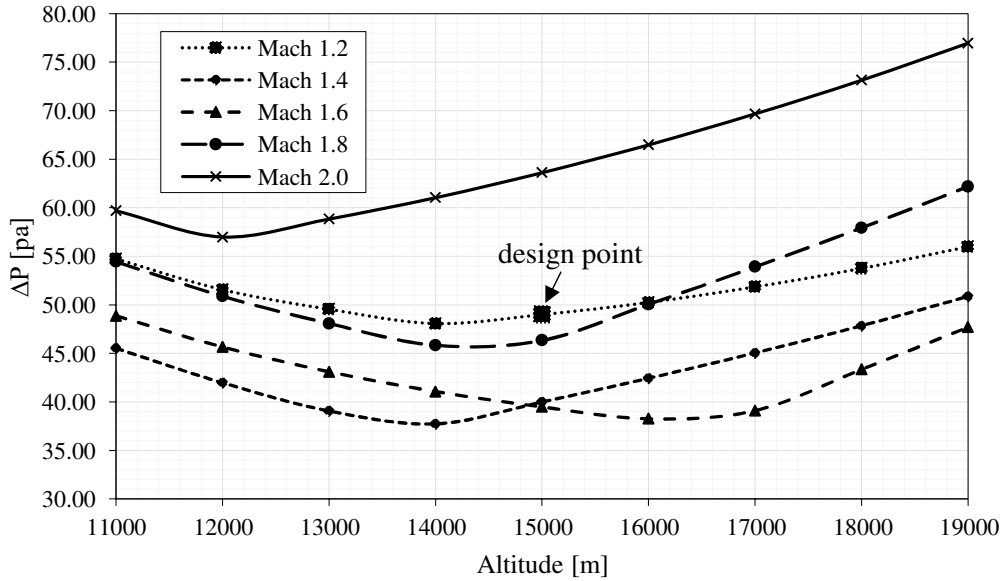

Fig. 16 Sonic boom intensity at different altitudes and Mach numbers

To explain the reason, the factors that influence the sonic boom intensity directly are investigated. From boom generation Eq. (**7**), the F-function due to volume and F-function due to lift have direct impact on the near-field pressure, which then influence the sonic boom intensity on the ground.

The lift coefficients at different Mach numbers and altitudes are plotted in Fig. 17. These are the required C_L to maintain level flight at different flight conditions. As the altitude increases, the air density decreases; therefore, the required C_L increases. The same principle applies to the Mach numbers.
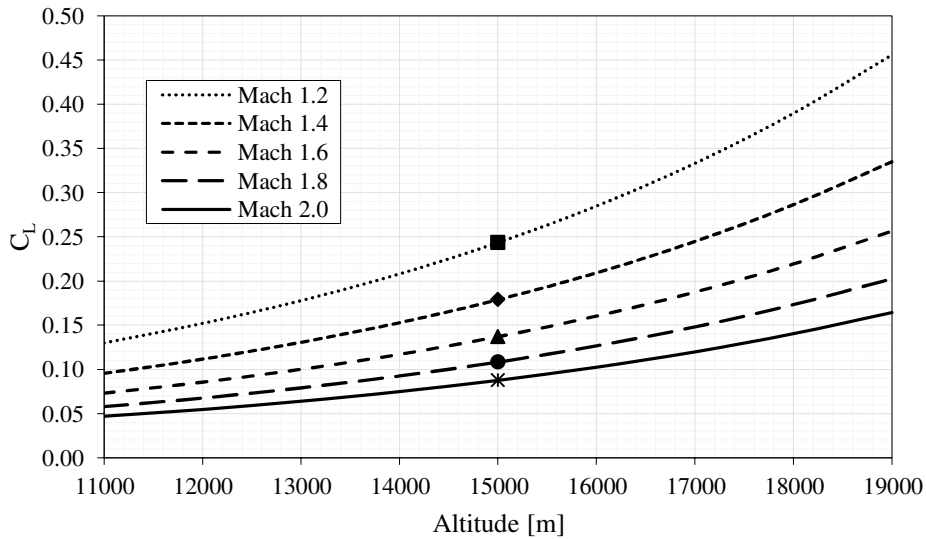
Fig. 17 Cruise lift coefficient at different altitudes and Mach numbers

The impact of C_L on the lift distribution and F-function due to lift are then plotted in Fig. 18(a) and Fig. 18 (b). It can be understood that, for a fixed design, the lower the Mach number, the higher the C_L. A higher C_L then leads to a higher peak in the F-function due to lift, which is then added to the total F-function.
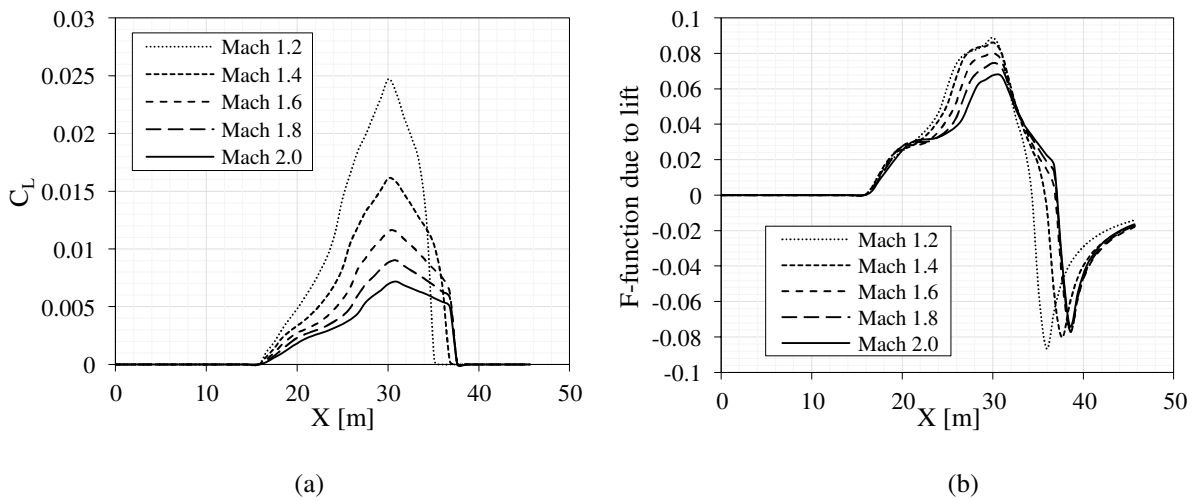

(a)

(b)

Fig. 18 Lift effect on sonic boom (a) lift coefficient and (b) F-function due to lift at different Mach numbers at 15000 m

On the other hand, the volume distributions varies with Mach numbers, as plotted in Fig. 19(a). That is because the cross-section Mach plane angles are different at different Mach numbers. The F-functions due to volume, as shown in Fig. 19(b), are then slightly different. All these differences are then added to the total F-function.
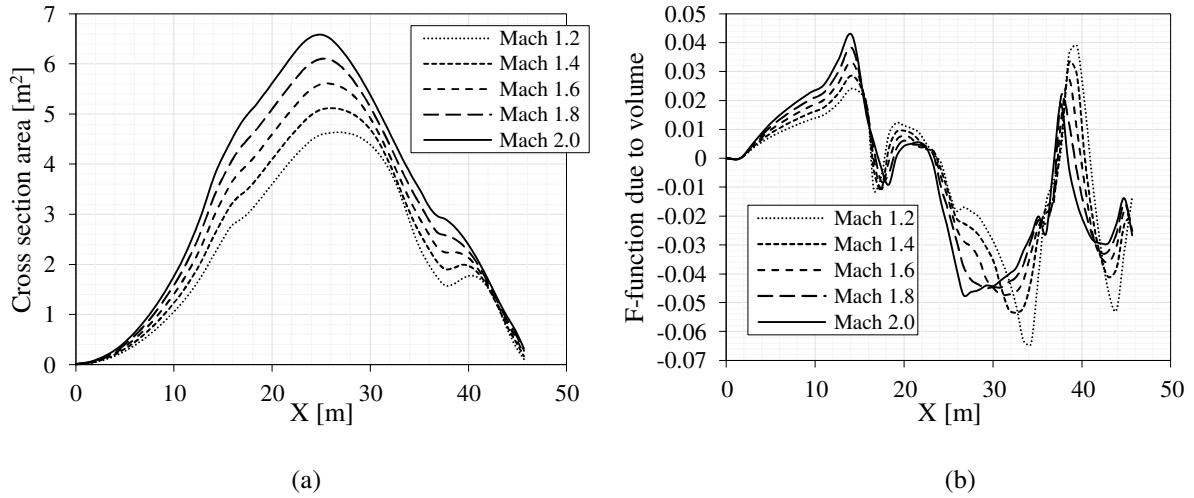
(a)   (b)

Fig. 19 Volume effect on sonic boom (a) cross section area and (b) F-function due to volume at different Mach

numbers at 15000 m

F-functions at different Mach numbers are plotted in Fig. 20, which indicates the near-field pressure levels according to Eq. **(8)**. The ground sonic boom intensity will have the same peaks as known from section 3.7.
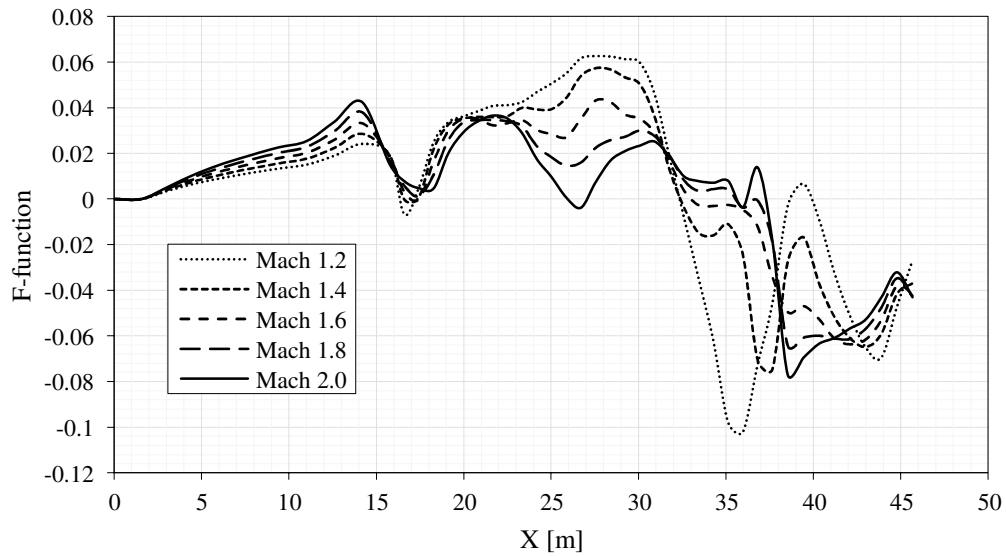

Fig. 20 F-functions at different Mach numbers at 15000 m

From the above analysis, it can be seen that the sonic boom intensity for a fixed design is more complex. This section can help the designer to get a more in-depth understanding of the sonic boom feature of a supersonic aircraft. Fig. 21 indicates the operational flexible zone under the assumed sonic boom limit of 1.0 psf (47.85 Pa).
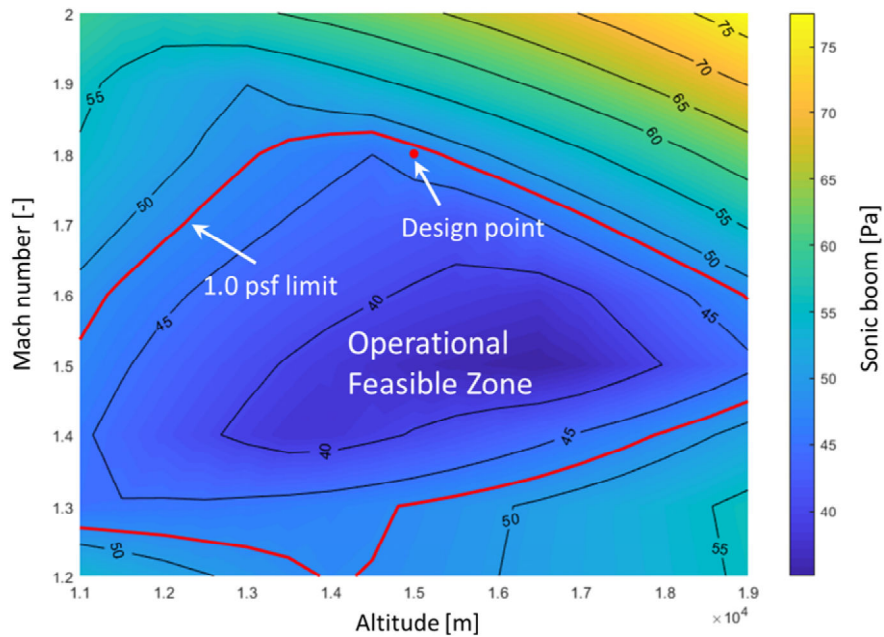
Fig. 21 Sonic boom limit operational feasible zone

5. Conclusions and Future Work

Through the study, a supersonic transport model is demonstrated in a multidisciplinary design analysis and optimization (MDAO) aircraft conceptual design environment. Within this model, the design of SSBJ concept is designed and optimized and the operational performances of the specific design are assessed.

The purpose of this paper is to study the operational performances of a fixed supersonic transport, which is seldomly studied before. Firstly, the sustained supersonic flights indicate there is an operational flexible zone limited by the maximum fuel capacity. For a cruise Mach number, there is a corresponding most fuel-efficient operating altitude. Further work still requires to explore the coordination of the design point and the most fuel-efficient point. Secondly, the combined supersonic and subsonic flight scenarios show that a high subsonic cruise subsegment can help to meet the current civil supersonic flight regulations and reduce the fuel consumption by 5.0% to 6.8%. However, the low supersonic (around cut-off Mach) cruise subsegments are both fuel-inefficient (6.3% - 8.1% increase) and time-inefficient (11.7% - 13.1% increase). Therefore, it is advised not to cruise near the cut-off Mach number region, if the design point is not in that region. Thirdly, the one-stop supersonic flight scheme can gain 47% to 53% time advantage over subsonic flight for long-range mission, which is attractive for high-end passengers. However, the supersonic transports, especially the business class, have tremendous fuel consumption (231 g/PAX/km) comparing

to the subsonic economy class (20 g/PAX/km). New environmental standards will be required for the return of supersonic transport. Lastly, the off-deign sonic boom performance is quite different from the common understanding. The sonic boom intensity does not necessarily decrease as the altitude increases and does not necessarily decrease as the Mach number decreases.

Declaration of Conflicting Interest

Funding

ORCID ID

Y Sun 0000-0001-7741-359X

H Smith 0000-0002-1573-9508

References

1. Sun Y, and Smith H. Review and Prospect of Supersonic Business Jet Design. *PROG AEROSP SCI*. 2017; 90: 12-38.

2. Smith H. A Review of Supersonic Business Jet Design Issues. *AERONAUT J*. 2007; 111: 761-76.

3. *Commercial Supersonic Technology: The Way Ahead*. Washington, D.C.: National Academy Press, 2001.

4. Sato K, Kumano T, Yonezawa M, et al. Low-Boom and Low-Drag Optimization of the Twin Engine Version of Silent Supersonic Business Jet. *Journal of Fluid Science and Technology*. 2008; 3: 576-85.

5. Minelli A, Salah el Din I, Carrier G, et al. Cooperation and Competition Strategies in Multi-objective Shape Optimization - Application to Low-boom/Low-drag Supersonic Business Jet. In: *31st AIAA Applied Aerodynamics Conference*, San Diego, California, 24-27 June 2013.

6. Banke J. NASA's Experimental Supersonic Aircraft Now Known as X-59 QueSST. NASA. 2018. https://www.nasa.gov/aero/nasa-experimental-supersonic-aircraft-x-59-quesst (accessed 20 August 2020).

7. Ohnuki T, Hirako K, Sakata K. National experimental supersonic transport project. In: *25th International Congress of the Aeronautical Sciences*, Hamburg, Germany, 3-8 September 2006.

8. Honda M, and Yoshida K. D-SEND project for low sonic boom design technology. In: *28th International Congress of the Aeronautical Sciences*, Brisbane, Australia, 23 - 28 September 2012.

9. Vermeersch O, Yoshida K, Ueda Y, et al. Natural laminar flow wing for supersonic conditions: Wind tunnel experiments, flight test and stability computations. *PROG AEROSP SCI*. 2015; 79: 64-91.

10. Liebhardta B, Lütjensb K, Tracyc RR, et al. Exploring the Prospect of Small Supersonic Airliners–A Business Case Study Based on the Aerion AS2 Jet. In: *17th AIAA Aviation Technology, Integration, and Operations Conference*, Denver, Colorado, 5-9 June 2017.

11. Hawkins AJ. This tiny supersonic jet could be the next generation Concorde. 2016. http://www.theverge.com/2016/11/15/13629104/boom-supersonic-jet-prototype-unveil-concorde (accessed 20 August 2020).

12. Gonzalez-Linero L. The Hoops on the Way to a Supersonic Business Jet (Performance Drivers for a Commercially Viable Product). In: *15th AIAA Aviation Technology, Integration, and Operations Conference*, Dallas, Texas, 22-26 June 2015.

13. Gonzalez Gallego O, Perez RE, Jansen PW. Technical Viability and Operational Assessment of a Supersonic Business Jet. In: *2018 Aviation Technology, Integration, and Operations Conference*, Atlanta, Georgia, 25-29 June 2018.

14. Liebhardt B, Linke F, Dahlmann K. Supersonic Deviations: Assessment of Sonic-Boom-Restricted Flight Routing. *J AIRCRAFT*. 2014; 51: 1987-96.

15. Wu Li, and Geiselhart K. Multidisciplinary Design Optimization of Low-Boom Supersonic Aircraft with Mission Constraints. *AIAA J*. 2021; 59: 165-79.

16. Kharina A, MacDonald T, Rutherford D. *Environmental Performance of Emerging Supersonic Transport Aircraft*. WORKING PAPER 2018-12, The International Council on Clean Transportation, 2018.

17. Lazzara DS, Magee T, Shen H, et al. Off-Design Sonic Boom Performance for Low-Boom Aircraft. In: *AIAA Scitech 2019 Forum*, San Diego, California, 7-11 January 2019.

18. Smith H, Sziroczák D, Abbe GE, et al. The GENUS Aircraft Conceptual Design Environment. *Proc IMechE Part G: J Aerospace Engineering*. 2018; 233: 2932-47.

19. Abbe GE. *Conceptual Design Methodologies for Small Solar Powered Unmanned Aerial Vehicle*. PhD Thesis, School of Aerospace Transport and Manufacturing, Cranfield University, Bedford, UK, 2015.

20. Sziroczak D. *Conceptual Design Methodologies Appropriate to Hypersonic Space and Global Transportation Systems*. PhD Thesis, School of Aerospace Transport and Manufacturing, Cranfield University, Bedford, UK, 2015.

21. Okonkwo PPC. *Conceptual Design Methodology for Blended Wing Body Aircraft*. PhD Thesis, School of Aerospace Transport and Manufacturing, Cranfield University, Bedford, UK, 2016.

22. Sun Y, and Smith H. Turbofan Airliner Conceptual Design in Multidisciplinary Design Analysis Optimization Environment. In: *1st International Conference in Aerospace for Young Scientists*, Beijing, P.R.China, 12-13 November 2016.

23. Sepulveda E, Smith H, Sziroczak D. Multidisciplinary Analysis of Subsonic Stealth Unmanned Combat Aerial Vehicles. *CEAS Aeronaut J*. 2018; 10: 431-42.

24. Sun Y, and Smith H. Supersonic Business Jet Conceptual Design in a Multidisciplinary Design Analysis Optimization Environment. In: *2018 AIAA/ASCE/AHS/ASC Structures, Structural Dynamics, and Materials Conference*, Kissimmee, Florida, 8-12 January 2018.

25. Sun Y, and Smith H. Sonic Boom and Drag Evaluation of Supersonic Jet Concepts. In: *2018 AIAA/CEAS Aeroacoustics Conference*, Georgia, Atlanta, 25-29 June 2018.

26. Sun Y, and Smith H. Low-boom low-drag solutions through the evaluation of different supersonic business jet concepts. *AERONAUT J*. 2019; 124: 76-95.

27. Sun Y, and Smith H. Low-boom low-drag optimization in a multidisciplinary design analysis optimization environment. *AEROSP SCI TECHNOL*. 2019; 94: 105387.

28. Saaris GR, Tinoco E, Lee J, et al. *A502I User's Manual-PAN AIR Technology Program for Solving Problems of Potential Flow about Arbitrary Configurations*. Boeing Document, Boeing, 1992.

29. Yuhara T, Makino Y, Rinoie K. Conceptual Design Study on Liquid Hydrogen-Fueled Supersonic Transport Considering Environmental Impacts. *J AIRCRAFT*. 2016; 53: 1168-73.

30. Kroo I, Willcox K, March A, et al. *Multifidelity Analysis and Optimization for Supersonic Design*. NASA/CR– 2010–216874, Langley Research Center, 2010.

31. Ueno A, Kanamori M, Makino Y. Multi-fidelity Low-boom Design Based on Near-field Pressure Signature. In: *54th AIAA Aerospace Sciences Meeting*, San Diego, California, 4-8 January 2016.

32. Gur O, Mason WH, Schetz JA. Full-Configuration Drag Estimation. *J AIRCRAFT*. 2010; 47: 1356-67.

33. Harris RV. *An Analysis and Correlation of Aircraft Wave Drag*. NASA TM X-947, National Technical Information Service, 1964.

34. EngineSim Version 1.8a. NASA Glenn Research Center. 2014. https://www.grc.nasa.gov/www/k-12/airplane/ngnsim.html (accessed 20 August 2020).

35. Whitham G. The Flow Pattern of A Supersonic Projectile. *Communications on Pure and Applied Mathematics*. 1952; 5: 301-48.

36. Thomas CL. *Extrapolation of Sonic Boom Pressure Signatures by the Waveform Parameter Method*. NASA TN D-6832, NASA Ames Research Center, 1972.

School of Aerospace, Transport and Manufacturing (SATM)   Staff publications (SATM)

2021-04-09

Design and operational assessment of a low-boom low-drag supersonic business jet

Sun, Yicheng

Sage